

# Strength degeneracy of LWAC and flexural behavior of LWAC members after fire

Chao-Wei Tang\*

Department Civil Engineering & Geomatics, Cheng Shiu University, No. 840, Chengcing Rd.,  
Niasong District, Kaohsiung City, Taiwan R.O.C.

(Received January 9, 2017, Revised April 7, 2017, Accepted April 10, 2017)

**Abstract.** The characteristics of lightweight aggregate (LWA) with a low specific gravity and high water absorption will significantly change the properties of lightweight aggregate concrete (LWAC). This study aimed at exploring the effect of presoaking degree of LWA on the strength degeneracy of LWAC and flexural behavior of LWAC members exposed to elevated temperatures. The residual mechanical properties of the LWAC subjected to elevated temperatures were first conducted. Then, the residual load tests of LWAC members (beams and slabs) after exposure to elevated temperatures were carried out. The test results showed that with increasing temperature, the decreasing trend of elastic modulus for LWAC was considerably more serious than the compressive strength. Besides, the presoaking degree of LWA had a significant influence on the residual compressive strength and elastic modulus for LWAC after exposure to 800°C. Moreover, owing to different types of heating, the residual load bearing capacity of the slab specimens were significantly different from those of the beam specimens.

**Keywords:** lightweight aggregate; reinforced concrete members; fire damage

## 1. Introduction

Lightweight aggregate concrete (LWAC) is made of lightweight aggregates (LWA) (Somayaji 2001). The use of LWAC in structures has many distinct advantages over normal weight aggregate concrete (NWC), such as reducing dead weight and increasing seismic performance (Lo *et al.* 1999, Young *et al.* 2002, Holm *et al.* 2004, Lo *et al.* 2004, Lo *et al.* 2008, Tang *et al.* 2011, Tang 2014, Hwang and Tran 2015, Ji *et al.* 2015, Oktay *et al.* 2015, Zhang *et al.* 2015, Vakhshouri and Nejadi 2016). These features are very suitable as a material for construction projects on Taiwan. Now days, for the sake of lightweight in order to reduce dead weight and seismic force, LWAC wall or floor are often used for high-rise buildings, and even all the members of the entire structure are made of LWAC (Chandra and Berntsson 2002).

Taiwan has established a fairly complete LWAC specification, including manufacturing technology, basic properties and application of technical regulations, and other information (Tang *et al.* 2011). In practical applications, however, construction technology has yet to attain complete. In particular, the characteristics of LWA with a low specific gravity and high water absorption (typically between 5 to 30%), which is often different from normal weight aggregates, will significantly change the properties of LWAC (Hammer 1990, Holm 1994, Hansen and Jensen 1995, BE96-3942/R20 2000, Holm *et al.* 2004, Liu and Zhang 2010). In other words, the water absorption

of LWA has a significant impact on the engineering properties and physical properties of LWAC. It is worth to explore the effect of LWA (light weight, high water absorption, etc.) on the engineering properties of LWAC.

Under the action of high temperature, the chemical composition, physical structure and water vapor content of concrete will change, leading to the decline of its mechanical properties. In general, the factors that affect the fire resistance of concrete include fire load (heating rate and maximum temperature), concrete properties (water content, permeability, type of aggregates), concrete types (ordinary, lightweight, and high strength concrete), and axial pressure. LWAs have the characteristics of porous, low density and high water absorption, so that the mechanical behavior and fire resistance of LWAC are different from NWC (Holm 1994, Chandra and Berntsson 2002). Under the standard temperature curve (ISO 834 standard fire curve), structural LWAC slabs, walls, and beams have demonstrated greater fire endurance periods than equivalent thickness members made with NWC (Holm 1994). However, the use of hydrocarbon combustion curve (hydrocarbon fire curve), fire test showed the opposite results. There have been a number of fire tests of LWAC in the literature (Copier 1983, Holm 1994, Chandra and Berntsson 2002, Wu *et al.* 2013, He *et al.* 2016, Karataş *et al.* 2017). However, these studies were mostly focused on the thermal and mechanical behavior of LWAC with low to medium strength (20 to 35 MPa) (Hammer 1990, Hansen and Jensen 1995). But, it is well known that the behavior of concrete becomes more brittle as its strength increases (Dong and Keru 2001, Yu *et al.* 2016). This effect is particularly evident with high strength concrete exposed to fire. In addition, there is relatively little research conducted on the strength degeneracy and structural behavior of LWAC members

---

\*Corresponding author, Professor  
E-mail: [tangcw@gcloud.csu.edu.tw](mailto:tangcw@gcloud.csu.edu.tw)

exposed to fire (Copier 1983). Therefore, there is an urgent need to establish a comprehensive fire protection design specifications or guidelines.

In view of the above, this study aims to explore the presoaking degree of LWA on the residual mechanical properties of LWAC subjected to elevated temperatures. Moreover, the strength degeneracy and flexural behavior of LWAC members (beams and slabs) after exposed to elevated temperatures were also investigated and compared with that of NWC members.

## 2. Experimental details

### 2.1 Experimental program

In this study, the effect of initial moisture conditions of the LWA on the on the hardened properties of concrete exposed to elevated temperatures was evaluated. The water content of the LWAC mixes was deliberately not adjusted in accordance with the absorption capacity of the aggregates to explore the effect of moisture condition of LWA on the properties of concrete after fire. The experimental work was divided into two main parts. The residual mechanical properties (i.e., compressive strength, elastic modulus, splitting strength, and flexural strength) of both the LWAC and NWC subjected to elevated temperatures were first conducted. Then, the residual load tests of LWAC and NWC members (beams and slabs) after exposure to elevated temperatures were carried out. In addition, the fireproof performance of the LWAC and NWC slabs was also explored and compared. The experimental variables include the presoaking degree of LWA (oven dry and pre-wetted for 30 min) and the maximum exposure temperatures, that is to say 400, 600, and 800°C.

### 2.2 Materials

Materials used for making specimens included cement, fine aggregates, coarse aggregates, superplasticizer, and reinforcing steel. The cement used complies with ASTM Type I Portland cement specifications. The fine aggregate was natural river sand and the coarse aggregate was crushed stone. The physical properties of the fine aggregate and the coarse aggregate are listed in Table 1. The lightweight coarse aggregate is a synthetic aggregate manufactured from fine sediments collected from the Shihmen Reservoir, which is one of Taiwan's major reservoirs. The physical and mechanical properties of the lightweight coarse aggregate are listed in Table 2. It can be seen that the lightweight coarse aggregate has a different particle size and its particle size ranges between 4.75 and 19 mm. In addition to aggregate size, the average particle density and water absorption of the lightweight coarse aggregates are also shown in Table 2. As can be seen from Table 2, the crushing strength of the LWA was 8.6 MPa, which was measured by compressing the aggregates in a steel cylinder through a prescribed distance of 20 mm in accordance with GB2842-81 (GB/T2842-81, China National Standard Test method for lightweight aggregates). The reinforcing bars

used included No. 3 and No. 4. The physical and mechanical properties of these reinforcing bars are shown in Table 3.

### 2.3 Mix proportions

In addition to the experimental group of LWAC, NWC was also prepared as the control group. Table 4 presents the mix proportions for both types of concrete. The specified 28-day compressive strength was chosen equal to 40 MPa. For example, the N40 is for the NWC. Two series of LWAC mixes with a nominal water-cement ratio of 0.44 made of LWA with different moisture states were prepared. As shown in Table 4, the L40 is for the LWAC with LWA presoaked in water for 30 minutes; while the LD40 is for the LWAC with oven-dried LWA.

The natural river sand and crushed stone were prepared in a saturated surface dry condition before use, while the LWAs were oven-dried and presoaked in water for 30 minutes, respectively. The treated aggregates were then stored indoors, in which the ambient temperature and relative humidity were controlled at  $25\pm 3^\circ\text{C}$  and  $50\pm 5\%$  to prevent moisture changes. In mixing, the cement, fine aggregates, and coarse aggregates were blended first, and then water and superplasticizer (if any) were added. The mixing continued until there was a uniform distribution of the materials.

Table 1 Physical property of normal weight aggregates

Type	Specific gravity (SSD)*	Water absorption (SSD)	Unit weight (dry-rodded) (kg/m <sup>3</sup> )	FM
Coarse aggregate	2.63	1.24%	1532	-
Fine aggregate	2.56	1.33%	-	2.75

Notes: SSD=Saturated surface dry condition; FM= Fineness modulus

Table 2 Physical and mechanical properties of lightweight aggregate

Sieve sizes (mm)	Particle density (OD) (g/cm <sup>3</sup> )	Water absorption (%)		Crushing strength (MPa)
		30 min.	24 hr.	
4.75-19	1.63	3.74	10.58	8.6

Note: OD=Oven dry condition

Table 3 Properties of steel bar

Steel bar	Cross sectional area (mm <sup>2</sup> )	Yield strength (MPa)	Yield strain	Tensile strength (MPa)
No. 3 Deformed bar	71.25	400	0.00215	582
No. 4 Deformed bar	132.73	411	0.00223	593

Table 4 Mix proportions of concrete

Mix No.	w/c	Cement (kg/m <sup>3</sup> )	Water (kg/m <sup>3</sup> )	Water (30 min) <sup>a</sup> (kg/m <sup>3</sup> )	Aggregate (kg/m <sup>3</sup> )		SP (kg/m <sup>3</sup> )	Unit weight (kg/m <sup>3</sup> )	Slump (cm)
					FA	CA			
N40	0.52	377	196	-	718	1024	0	2315	11
L40	0.44	480	211	23	634	606	1.44	1955	10
LD40	0.44	480	211	-	634	606	1.44	1932	8

Notes: a=Water in quantity equal to half an hour's aggregate absorption. FA=Fine aggregate; CA=Coarse aggregate; SP=Superplasticizer

## 2.4 Casting of specimens

The details of the beam specimens and their reinforcement layouts are shown in Fig. 1. The beams were 1.5 m long with a rectangular cross section of 150 × 200 mm. The arrangement of the reinforcing steel was the same for all beams. No. 4 deformed bars and No. 3 deformed bars were used for longitudinal and transverse reinforcement, respectively. Eight beam specimens were fabricated for each concrete mixture. Two beams were used for static load capacity tests, and the other beams were used for residual load tests after exposure to elevated temperatures. On the other hand, Fig. 2 shows the details of the slab specimens and their reinforcement layouts. The slabs were 1.2 m long with a rectangular cross section of 150 × 400 mm. As can be seen in Fig. 2, No. 4 deformed bars were used for longitudinal reinforcement, while No. 3 deformed bars were used for transverse reinforcement. Eight slab specimens were fabricated for each concrete mixture. Two slab specimens were used for static load capacity tests, and the other slab specimens were used for residual load tests after exposure to elevated temperatures.

Concrete specimens for each test were cast out of each mix and compacted using an external vibrator. Along with each mix, enough cylindrical specimens (150 mm in diameter and 300 mm high) were cast for compressive strength test, elastic modulus test, and splitting strength test of concrete; eight prism specimens (360 mm length × 100 mm width × 100 mm thickness) were cast for flexural strength of concrete. Following casting, all the specimens were covered overnight with a wet hessian and polyethylene sheets for a period of 24 hours. After 24 hours, all specimens were removed from the molds. To maintain the same environmental conditions, all specimens were placed in a water bath in the laboratory. After curing, the specimens were removed from the water bath three days before the test.

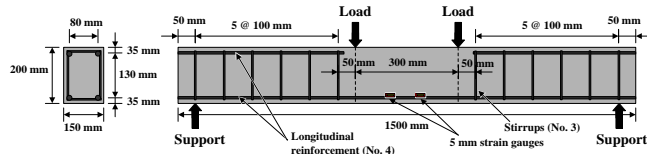


Fig. 1 Cross-sections and dimensions of beam specimens

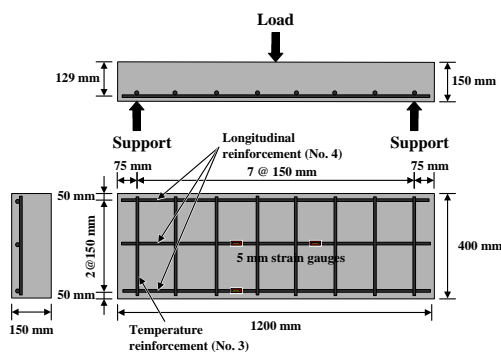
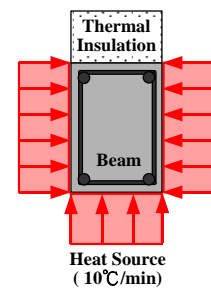


Fig. 2 Cross-sections and dimensions of slab specimens

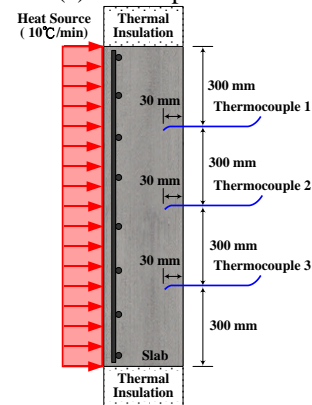
## 2.5 Testing methods and instrumentation

In the study, beam specimens were exposed to three-sided heating, while slab specimens were exposed to single-sided heating, as shown in Fig. 3. The members and cylindrical specimens were heated without preload at a prescribed rate (10°C/min) until the temperature inside the furnace reached the target temperatures. When the targeted maximum temperature was reached, the furnace temperature was maintained for another three hours to achieve a thermal steady state in the whole specimen. The furnace was then shut off, and the specimens were allowed to cool slowly in the furnace with the door opened. After cooling to room temperature, the residual strength tests were carried out on the members and cylindrical specimens. The tests of compressive strength, elastic modulus, splitting tensile strength and flexural strength for concrete were performed according to ASTM C39, ASTM C469, ASTM C496 and ASTM C78 standards, respectively.

A hydraulic servo-controlled testing machine was used in both the load capacity tests and the residual load tests of the LWAC and NWC members (beams and slabs). Beam specimens were tested using a four-point loading method with a shear-span-to-depth ratio ( $a/d$ ) of 3.33, while slab specimens were tested using a three-point loading method with  $a/d$  of 4.07. The specimens' deflections at midspan were measured by linear variable differential transducers (LVDTs). The entire test progress was monitored on a computer screen. In addition, the outputs of the LVDTs, the load cell (actuator force) and the stroke of the testing machine were collected and stored on a diskette via a data logger.



(a) Beam specimens



(b) Slab specimens

Fig. 3 Heating method for specimens

### 3. Experimental results and discussion

#### 3.1 Residual mechanical properties of LWAC after fire

##### 3.1.1 Residual compressive strength and elastic modulus

The compressive strength versus temperature curve for each concrete mix is shown in Fig. 4. After exposure to different temperatures, the compressive strength for the N40 ranged from 12.5 to 44.0 MPa, while the compressive strength for the L40 and LD40 ranged from 19.9 to 44.0 MPa and from 16.0 to 50.1 MPa, respectively. At room temperature, the compressive strength of the L40 was less than that of the LD40. This is mostly because that for a fixed amount of cement in the L40, the water/cement ratio of cement paste was decreased by using over-dried LWA. In other words, owing to high water absorption of the LWA, the actual water-cement ratio was lower than its nominal value, thus resulting in a stronger cement matrix. As a result, the strength of the resulting concrete was increased. In addition, Fig. 4 shows that the residual compressive strength of each concrete mix decreased with increasing target temperature in fire test. On the whole, the residual compressive strength of LWAC was higher than that of NWC. At a temperature of 400°C, the residual compressive strength of each concrete mix can maintain about 95% of the strength at room temperature. With a further increase in temperature to 600°C, the residual compressive strength of each concrete mix can still maintain about 80% of the room-temperature strength. However, once the temperature was raised to 800°C, the residual compressive strength for the LD40 dropped by 68% as compared with the room-temperature strength, while the residual compressive strength for the L40 only dropped by 55% as compared with the room-temperature strength. This is due to the fact that there was a relatively dense microstructure of the matrix in the LD40 with oven-dried LWA, which resulted in the greater the internal vapor pressure. In other words, the higher the probability of spalling of the LD40 specimen, and thus its strength decline was greater than that of the L40 specimen.

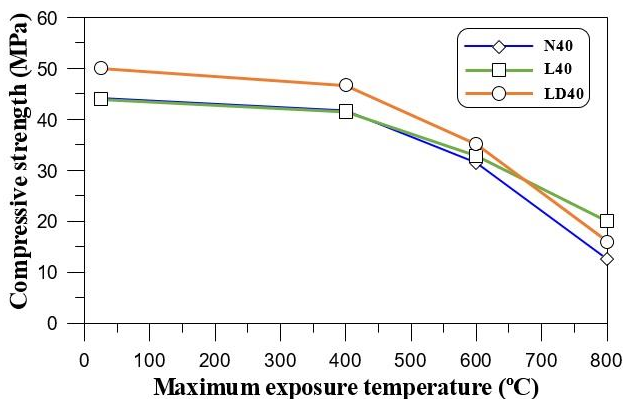


Fig. 4 Compressive strength versus temperature curves for cylindrical specimens

On the other hand, Fig. 5 shows the elastic modulus versus temperature curve for each concrete mix. With the increase of temperature, the decreasing trend of elastic modulus was obviously more serious than the compressive strength. This is because that the elastic modulus is more sensitive to cracks at either the macro- or micro-scale caused by high temperatures (Hsu *et al.* 1963). As can be seen in Fig. 5, after exposure to different temperatures, the elastic modulus for the N40 ranged from 1.2 to 30.2 GPa, while the elastic modulus for the L40 and LD40 ranged from 4.8 to 23.2 GPa and from 2.8 to 24.3 GPa, respectively. At room temperature, the elastic modulus of the L40 was a little less than that of the LD40. But the magnitudes of modulus of the L40 and LD40 were significantly lower than that of the N40. Moreover, it can also be seen in Fig. 5, the residual elastic modulus of each concrete mix decreased with increasing temperature in fire test. On the whole, the residual elastic modulus of the LWAC was higher than that of the NWC. At a temperature of 400°C, the residual elastic modulus of each concrete mix can maintain about 80% of the room-temperature strength. With a further increase in temperature to 600°C, the residual elastic modulus of each concrete mix can still maintain about 46% of the room-temperature strength. But after exposure to 800°C, the residual elastic modulus of the N40 was 96% lower than the room-temperature strength, while the residual elastic modulus of the L40 and LD40 only dropped by 79 and 88%, respectively, as compared with the room-temperature strength.

##### 3.1.2 Residual splitting strength and flexural strength

Fig. 6 shows the splitting strength versus temperature curve for each concrete mix. With increasing temperature, the change of splitting strength was inconsistent with the results of the compressive strength. The results show that the influence of high temperature on the compressive strength and split strength of concrete is different. As can be seen in Fig. 6, after exposure to different temperatures, the splitting strength for the N40, L40, and LD40 ranged from 0.6 to 3.7 MPa, from 0.7 to 2.7 MPa, and from 0 to 3.0 MPa, respectively. At temperature 400°C, the LWAC and NWC specimens reached peak strength.

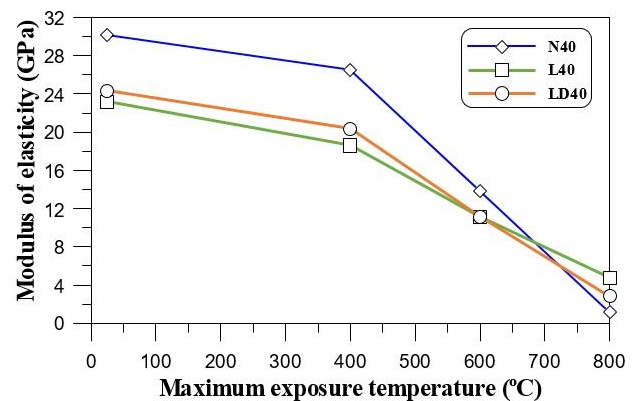


Fig. 5 Elastic modulus versus temperature curves for cylindrical specimens

This is because the temperature inside the test specimen was still lower than 400°C although the furnace temperature was maintained for three hours. In other words, the average temperature of the test specimen had not yet reached 400°C. However, owing to rapid drying of the specimen exposed to high temperature, the moisture in matrix pores can be easily evaporated (Siddique and Kaur 2012). As a result, the residual splitting strength increased. The residual splitting strength of the N40, L40, and LD40 increased by 27, 3.8, and 20%, respectively, compared to the room temperature value. But the residual splitting strength of each concrete mix decreased significantly after being exposed to 600 °C for three hours. In particular, after exposure to 800 °C, the residual splitting strength of the N40, L40, and LD40 dropped by 78, 73, and 100%, respectively, as compared with the room-temperature strength.

On the other hand, the flexural strength (i.e., modulus of rupture) versus temperature curve for each concrete mix was shown in Fig. 7. In general, the change of flexural strength with increasing temperature was consistent with the results of the splitting strength. As can be seen in Fig. 7, after exposure to different temperatures, the flexural strength of the N40, L40, and LD40 ranged from 1.6 to 10.4 MPa, from 0 to 9.8 MPa, and from 0 to 8.2 MPa, respectively. At temperature 400°C, the LWAC and NWC specimens reached peak strength.

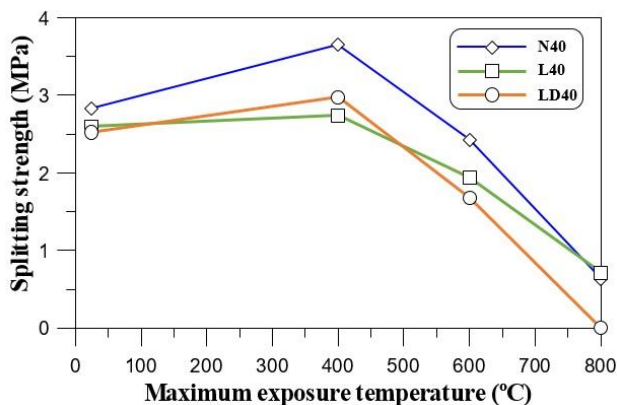


Fig. 6 Splitting strength versus temperature curves for cylindrical specimens

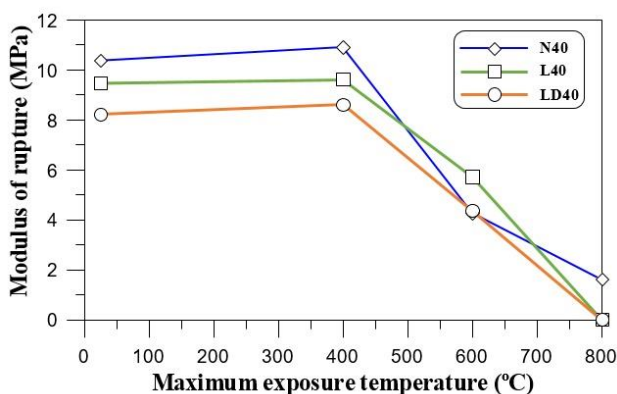


Fig. 7 Flexural strength versus temperature curves for prismatic specimens

The residual flexural strength of the N40, L40, and LD40 increased by 4.7, 2.3, and 0%, respectively, compared to the room temperature value. The reason for this result has been mentioned above. Overall, at 400°C, the increase in residual flexural strength was not significant. However, after being exposed to 600°C for three hours, the residual flexural strength of each concrete mix decreased significantly.

Especially, after exposure to 800°C, the residual flexural strength of the N40 dropped by 85%, as compared with the room-temperature strength; while the residual flexural strength of the L40 and LD40 dropped by 100%, as compared with the room-temperature strength.

### 3.2 Residual flexural behavior of LWAC members after fire

#### 3.2.1 Residual load bearing capacity of LWAC beams

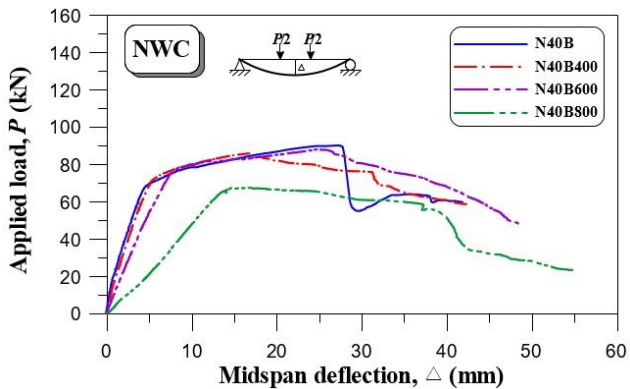
The load versus midspan deflection curves obtained from the residual load tests of the LWAC and NWC beams after exposure to elevated temperatures were displayed in Fig. 8. On the whole, the initial slope of ascending branches decreased with increasing temperature. In addition, after reaching its ultimate load, the load dropped suddenly. Then, the curve gradually became flatter and more extended until the concrete crushed. At room temperature, the toughness (i.e. the area under the load versus deflection curve up to fracture) of the LWAC beams (L40B and LD40B) is relatively lower than that of the NWC beam (N40B). At temperature 400°C, the load versus midspan deflection curves were quite in close agreement with those of the LWAC and NWC beams tested at room temperature until they started failing under the applied loads. With a further increase in temperature to 600°C, the initial slope of the load versus midspan deflection curves of the NWC and LWAC beams (N40B600, L40B600, and LD40B600 in Fig. 8) decreased obviously. In fact, the decrease of slope on the load versus midspan deflection curves implies that the stiffness of the beam members was slightly reduced. Especially, after being exposed to 800°C for three hours, the initial slope of ascending branches decreased significantly. In other words, the stiffness of the beam members was also reduced. Moreover, the residual load bearing capacity (i.e., residual strength) of the NWC and LWAC beams (N40B800, L40B800, and LD40B800 in Fig. 8) decreased dramatically. As can be seen in Fig. 8, the residual strength for N40B800, L40B800, and LD40B800 decreased from 90.1 to 67.6 kN, from 86.7 to 65.2 kN, and from 86.5 to 65.5 kN, respectively. The residual strength of the N40B800 dropped by 25.0%, as compared with the room-temperature strength; while the residual strength of the L40B800 and LD40B800 dropped by 24.8 and 24.3%, respectively, as compared with the room-temperature strength. Therefore, the effect of the presoaking degree of LWA on flexural behavior of LWAC beam after fire did not differ significantly.

In addition, according to the ACI 318 specification, the allowable deflection is  $L/180$  for flat roofs not supporting or attached to nonstructural elements likely to be damaged by large deflection. Therefore, the maximum allowable

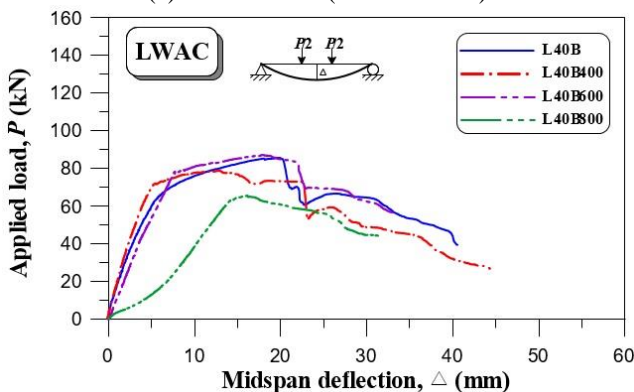
deflection of the beam is 7.8 mm. It can be seen from Fig. 8 that the deflections of the NWC and LWAC beams at the yielding load were less than 7.8 mm at room temperature or high temperature.

### 3.2.2 Residual load bearing capacity of LWAC slabs

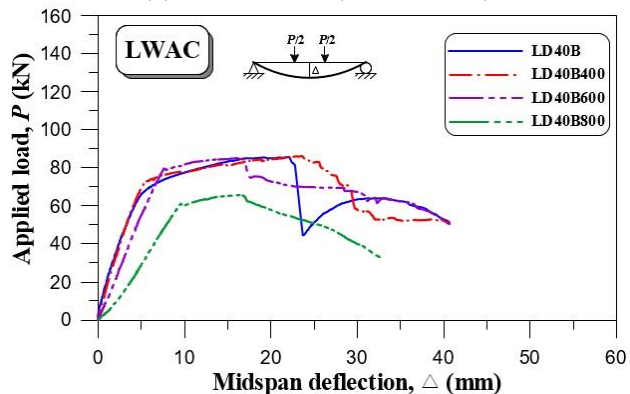
Fig. 9 shows the load versus midspan deflection curves obtained from the residual load tests of the LWAC and NWC slabs after exposure to elevated temperatures. At room temperature, the toughness of the LWAC slabs (L40S and LD40S) is relatively lower than that of the NWC slab (N40S).



(a) NWC beams (Mix No. N40)



(b) LWAC beams (Mix No. L40)



(c) LWAC beams (Mix No. LD40)

Fig. 8 Load versus midspan deflection curves for beams

This result was similar to those of the beam specimens. However, it can be clearly seen in Fig. 9, the influence of temperature on the initial slope of ascending branches was not significant. Moreover, with the increase in temperature of the fire tests, the ductility of the slab specimen was gradually reduced, and thus resulting in a brittle failure mode. At 400 and 600°C, after reaching its ultimate strength, the load decreased sharply until it reached a plateau value and then followed a smoother decreasing trend. In particular, heated to 800°C, after reaching its ultimate strength, the load decreased rapidly. These results were significantly different from those of the beam specimens. The reason may come from different types of heating, so that the slabs had a large temperature gradient.

In addition, Fig. 9 shows that the residual strength of the N40S800, L40S800, and LD40S800 decreased from 119.7 to 95.6 kN, from 113.0 to 97.0 kN, and from 113.5 to 89.7 kN, respectively. The residual strength of the N40S800 dropped by 20.1%, as compared with the room-temperature strength; while the residual strength of the L40S800 and LD40S800 dropped by 14.2 and 21.0%, respectively, as compared with the room-temperature strength. Accordingly, the effect of the presoaking degree of LWA on flexural behavior of LWAC slab after fire was significant. Similarly, according to the ACI 318 specification, the allowable deflection is  $L/180$  for flat roofs not supporting or attached to nonstructural elements likely to be damaged by large deflection. Therefore, the maximum allowable deflection of the slab is 4.4 mm. It can be seen from Fig. 9 that the resulted deflections of the NWC and LWAC slabs at the yielding load did not exceed the maximum allowable deflection of the ACI code.

On the other hand, Fig. 10 shows the measured temperature versus time curves for unexposed surfaces of slab specimens. As can be seen in Fig. 10, the temperature for unexposed surfaces of slab specimens rose at a uniform rate within the first hour and then followed a steeper increasing trend. Moreover, the temperature rise rate on the unexposed surface in the LWAC slabs were mostly slower compared with the NWC slabs due to the lower heat conductivity of the LWAC.

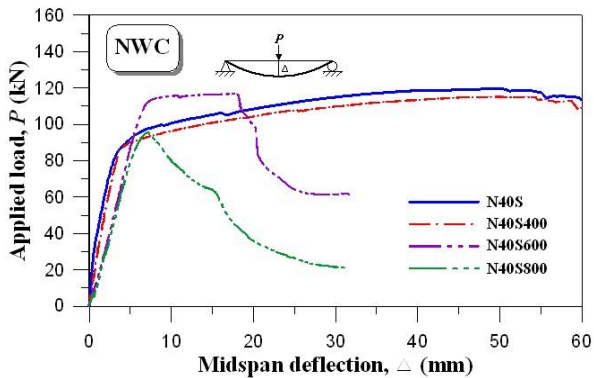
According to ASTM-E119, the average temperature rise at the unexposed surface of the specimen shall not exceed 139°C. Fig. 10 shows that the average temperature increased at the unexposed concrete surface remained less than 139°C for all slabs tested. At a temperature of 400, 600, and 800°C, the average temperatures for unexposed surfaces of slab specimens were 91.7, 109.8 and 120.5°C for the N40; 77.3, 86.9 and 98.4°C for the L40; 83.9, 92.5 and 102.8°C for the LD40, respectively. Thus, the experimental data demonstrate that failure by the unexposed surface temperature criterion did not occur for any of the slabs. Further, in spite of the presoaking degree of LWA, the LWAC slabs exhibited almost the same trend in terms of the evolution of their fireproof performance. In other words, the effect of the presoaking degree of LWA on fireproof performance of LWAC slab in fire did not differ significantly.

4. Conclusions

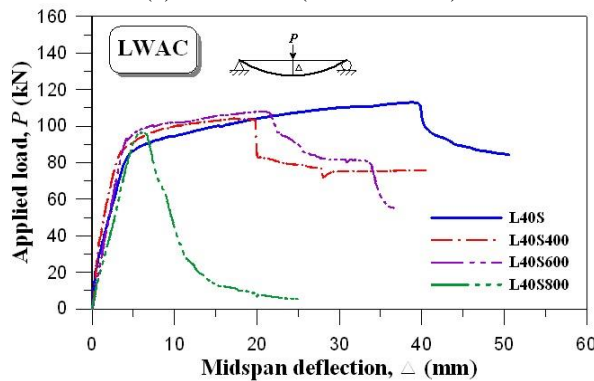
Based on the experimental results, the following conclusions can be drawn:

- With increasing temperature, the decreasing trend of elastic modulus of the LWAC was considerably more serious than the compressive strength. Besides, the presoaking degree of LWA had a significant influence on the residual compressive strength and elastic modulus of the LWAC after exposure to 800°C.
- With increasing temperature, the change of flexural strength of the LWAC was consistent with the splitting strength. But the trend of splitting strength and flexural strength was inconsistent with the compressive strength. In particular, after exposure to 800°C, the residual splitting strength of the N40, L40, and LD40 dropped by 78, 73, and 100%, respectively, as compared with the room-temperature strength.

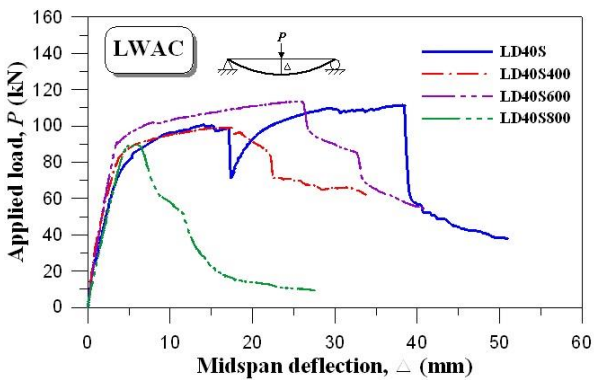
- After being exposed to 800°C for three hours, the residual load bearing capacity of the NWC and LWAC beams decreased dramatically. The residual strength of the N40B800 dropped by 25.0%, as compared with the room-temperature strength; while the residual strength of the L40B800 and LD40B800 dropped by 24.8 and 24.3%, respectively, as compared with the room-temperature strength. Therefore, the effect of the presoaking degree of LWA on flexural behavior of LWAC beam after fire did not differ significantly.
- After being exposed to 800°C for three hours, the residual load bearing capacity of the NWC and LWAC slabs decreased significantly. The residual strength of the N40S800 dropped by 20.1%, as compared with the room-temperature strength; while the residual strength of the L40S800 and LD40S800 dropped by 14.2 and 21.0%, respectively, as compared with the room-temperature strength. Accordingly, the effect of the presoaking degree of LWA on flexural behavior of the LWAC slab after fire was significant.



(a) NWC slab (Mix No. N40)

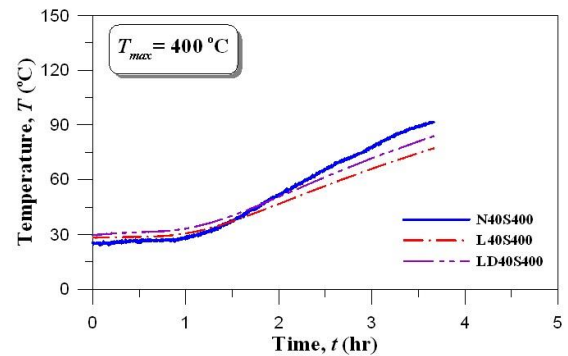


(b) LWAC slab (Mix No. L40)

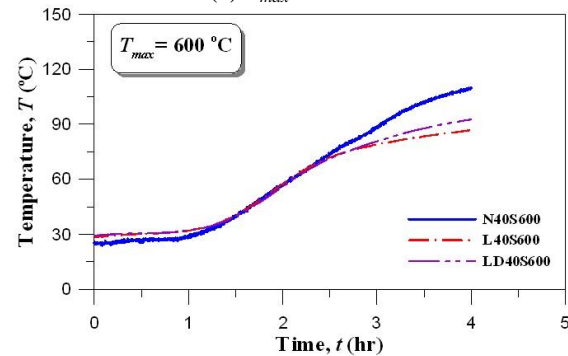


(c) LWAC slab (Mix No. LD40)

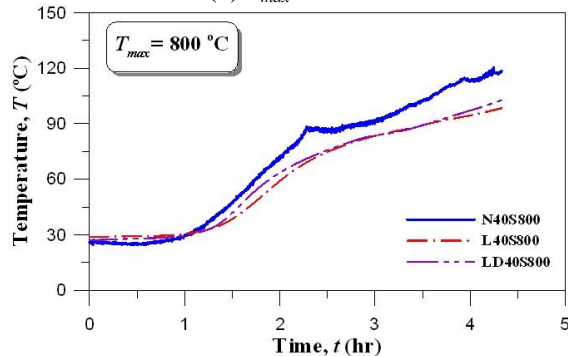
Fig. 9 Load versus midspan deflection curves for slabs



(a)  $T_{max}=400^{\circ}\text{C}$



(b)  $T_{max}=600^{\circ}\text{C}$



(c)  $T_{max}=800^{\circ}\text{C}$

Fig.10 Temperature-time curve for unexposed surfaces of slab specimens

- The residual load bearing capacity of the slab specimens were significantly different from those of the beam specimens. The reason may come from different types of heating, so that the slabs had a large temperature gradient.
- In spite of the presoaking degree of LWA, the LWAC slabs exhibited almost the same trend in terms of the evolution of their fireproof performance. Therefore, the effect of the presoaking degree of LWA on fireproof performance of the LWAC slab in fire did not differ significantly.

## Acknowledgments

The author expresses his gratitude and sincere appreciation to the Ministry of Science and Technology, Taiwan, for financing this research work.

## References

- ACI 318-14 (2014), *Building Code Requirements for Structural Concrete and Commentary*, American Concrete Institute.
- ASTM C39/C39M-14a (2014), *Standard Test Method for Compressive Strength of Cylindrical Concrete Specimens*, ASTM International, West Conshohocken, Pennsylvania, U.S.A.
- ASTM C469/C469M-14 (2014), *Standard Test Method for Static Modulus of Elasticity and Poisson's Ratio of Concrete in Compression*, ASTM International, West Conshohocken, Pennsylvania, U.S.A.
- ASTM C496-96 (1996), *Standard Test Method for Splitting Tensile Strength of Cylindrical Concrete Specimens*, ASTM International, West Conshohocken, Pennsylvania, U.S.A.
- ASTM C78/C78M-10 (2010), *Standard Test Method for Flexural Strength of Concrete (Using Simple Beam with Third-Point Loading)*, ASTM International, West Conshohocken, Pennsylvania, U.S.A.
- BE96-3942/R20 (2000), *The Effect of the Moisture History on the Water Absorption of Lightweight Aggregates*, EuroLightCon.
- Chandra, S. and Berntsson, L. (2002), *Lightweight Aggregate Concrete*, Noyes Publications, New York, U.S.A.
- CNS 7332 (2007), *Method of Determination for Thermal Conductivity of Heat Insulating Materials by Means of Comparison with a Standard Plate of Known Conductivity*, Bureau of Standards, Metrology and Inspection, M.O.E.A., R.O.C..
- Copier, W.J. (1983), "The spalling of normal weight and lightweight concrete exposed to fire", *J. Am. Concrete Inst.*, **80**(4), 352-353.
- Dong, Z. and Keru, W. (2001), "Fracture properties of high-strength concrete", *J. Mater. Civil Eng.*, **13**(1), 86-88.
- Galle, C. (2001), "Effect of drying on cement-based materials pore structure as identified by mercury intrusion porosimetry—a comparative study between oven-, vacuum-, and freeze-drying", *Cement Concrete Res.*, **31**(10), 1467-1477.
- GB/T2842-81 (1981), *Test Method for Lightweight Aggregates*, China National Standard.
- Hammer, T.A. (1990), *Marine Concrete Structures Exposed to Hydrocarbon Fire-Spalling Resistance of LWA Concrete*, SINTEF-Report No. STF65 A88064, Trondheim, 8.
- Hansen, P.A. and Jensen, J.J. (1995), *Fire Resistance and Spalling Behavior of LWA Beams, Report 6.3, High Strength Concrete phase 3*, SINTEF-Report No. STF70 A95004, Trondheim, 13.
- He, K.C., Guo, R.X., Ma, Q.M., Yan, F., Lin, Z.W. and Sun, Y.L. (2016), "Experimental research on high temperature resistance of modified lightweight concrete after exposure to elevated temperatures", *Adv. Mater. Sci. Eng.*, **6**.
- Holm, T.A. (1994), *Lightweight Concrete and Aggregates*, Standard Technical Publication 196C.
- Holm, T.A., Ooi, O.S. and Bremner, T.W. (2004), *Moisture Dynamics in Lightweight Aggregate and Concrete*, Expanded Shale Clay & Slate Institute.
- Hsu, T.T.C., Slate, F.O., Sturman, G.M. and Winter, G. (1963), "Microcracking of plain concrete and the shape of the stress-strain curve", *ACI Mater. J.*, **60**(2), 209-224.
- Hwang, C.L. and Tran, V.A. (2015), "A study of the properties of foamed lightweight aggregate for self-consolidating concrete", *Constr. Build. Mater.*, **87**, 78-85.
- Ji, T., Zheng, D.D., Chen, X.F., Lin, X.J. and Wu, H.C. (2015), "Effect of prewetting degree of ceramicsite on the early-age autogenous shrinkage of lightweight aggregate concrete", *Constr. Build. Mater.*, **98**, 102-111.
- Karataş, M., Balun, B. and Benli, A. (2017), "High temperature resistance of self-compacting lightweight mortar incorporating expanded perlite and pumice", *Comput. Concrete*, **19**(2), 121-126.
- Liu, X. and Zhang, M.H. (2010), "Permeability of high-performance concrete incorporating presoaked lightweight aggregates for internal curing", *Mag. Concrete Res.*, **62**(2), 79-89.
- Lo, Y., Gao, X.F. and Jeary, A.P. (1999), "Microstructure of pre-wetted aggregate on lightweight concrete", *Build. Environ.*, **34**(6), 759-764.
- Lo, Y., Cui, H.Z. and Li, Z.G. (2004), "Influence of aggregate prewetting and fly ash on mechanical properties of lightweight concrete", *J. Waste Manage.*, **24**(4), 333-338.
- Lo, Y., Cui, H.Z., Tang, W.C. and Leung, W.M. (2008), "The effect of aggregate absorption on pore area at interfacial zone of lightweight concrete", *Constr. Build. Mater.*, **22**(4), 623-628.
- Oktay, H., Yumrutas, R. and Akpolat, A. (2015), "Mechanical and thermophysical properties of lightweight aggregate concretes", *Constr. Build. Mater.*, **96**, 217-225.
- Siddique, R. and Kaur, D. (2012), "Properties of concrete containing ground granulated blast furnace slag (GGBFS) at elevated temperatures", *J. Adv. Res.*, **3**(1), 45-51.
- Somayaji, S. (2001), *Civil Engineering Materials*, Prentice Hall, Upper Saddle River, New Jersey, U.S.A.
- Tang, C.W., Chen, H.J., Wang, S.Y. and Spaulding, J. (2011), "Production of synthetic lightweight aggregate using reservoir sediments for concrete and masonry", *Cement Concrete Comp.*, **33**(2), 292-300.
- Tang, C.W. (2014), "Producing synthetic lightweight aggregates by treating waste TFT-LCD glass powder and reservoir sediments", *Comput. Concrete*, **13**(2), 149-171.
- Vakhshouri, B. and Nejadi, S. (2016), "Self-compacting lightweight concrete; mix design and proportions", *Struct. Eng. Mech.*, **58**(1), 143-161.
- Wu, X., Wu, Z.M., Zheng, J.J., Ueda, T. and Yi, S.H. (2013), "An experimental study on the performance of self-compacting lightweight concrete exposed to elevated temperature", *Mag. Concrete Res.*, **65**(13), 780-786.
- Young, J.F., Mindess, S. and Daewin, D. (2002), *Concrete*, Prentice-Hall, Inc., Upper Saddle River, New Jersey, U.S.A.
- Yu, K., Yu, J., Lu, Z. and Chen, Q. (2016), "Fracture properties of high-strength/high-performance concrete (HSC/HPC) exposed to high temperature", *Mater. Struct.*, **49**(11), 4517-4532.
- Zhang, J., Wang, J. and Han Y. (2015), "Simulation of moisture field of concrete with pre-soaked lightweight aggregate addition", *Constr. Build. Mater.*, **96**, 599-614.